Tree Physiology 37, 1713–1726
doi:10.1093/treephys/tpx093

Research paper

# PtoMYB170 positively regulates lignin deposition during wood formation in poplar and confers drought tolerance in transgenic Arabidopsis

Changzheng Xu[1,†], Xiaokang Fu[1,†], Rui Liu[1,†], Li Guo[1], Lingyu Ran[1], Chaofeng Li[2], Qiaoyan Tian[1], Bo Jiao[1], Bangjun Wang[1] and Keming Luo[1,2,3]

[1]Key Laboratory of Eco-environments of Three Gorges Reservoir Region, Ministry of Education, Chongqing Key Laboratory of Transgenic Plant and Safety Control, Institute of Resources Botany, School of Life Sciences, Southwest University, 400715 Chongqing, China; [2]Key Laboratory of Adaptation and Evolution of Plateau Biota, Northwest Institute of Plateau Biology, Chinese Academy of Sciences, 810008 Xining, China; [3]Corresponding author (kemingl@swu.edu.cn)

Received January 23, 2017; accepted June 22, 2017; published online July 28, 2017; handling Editor Janice Cooke

Wood formation is a complex developmental process under multi-level transcriptional control executed by a large set of transcription factors. However, only limited members have been characterized to be key regulators of lignin biosynthesis in poplar. Here we report the conserved and unique functions of PtoMYB170, a transcription factor identified from *Populus tomentosa* (Chinese white poplar), in lignin deposition and drought tolerance in comparison with its duplicate paralog PtoMYB216. *PtoMYB170* is preferentially expressed in young leaves and xylem tissues. Overexpression of *PtoMYB170* in transgenic poplar plants resulted in stronger lignification and more thickened secondary wall in xylem compared with wild-type plants, whereas the CRISPR/Cas9-generated mutation of *PtoMYB170* weakened lignin deposition, thereby leading to a more flexible and collapsed xylem phenotype. Transient expression experiments demonstrated that PtoMYB170 specifically activated the expression of lignin biosynthetic genes, consistent with the function of PtoMYB216. However, GUS staining assays revealed that *PtoMYB170* was specifically expressed in guard cells of transgenic Arabidopsis while *PtoMYB216* was not. Heterologous expression of *PtoMYB170* in Arabidopsis enhanced stomatal closure in the dark and resulted in drought tolerance of the transgenic plants through reduced water loss, indicating a diversified role from *PtoMYB216*. These results revealed the *PtoMYB170*-dependent positive transcriptional regulation on lignin deposition in poplar and its coordinated function in enhancing drought tolerance by promoting dark-induced stomatal closure.

***Keywords***: drought tolerance, MYB transcription factor, *Populus tomentosa*, stomatal aperture, wood formation.

## Introduction

Wood dominates biomass accumulation in terrestrial ecosystems and also possesses important economic values as feedstock for timber, pulping, paper and biofuel production (Ragauskas et al. 2006, Bonan 2008). Wood formation mainly derives from secondary xylem development and requires lignin deposition giving rise to a highly thickened cell wall of xylem fibers and vessels (Zhang et al. 2014). Lignin is a phenolic polymer composed of three types of monolignol units that include coniferyl alcohol, sinapyl alcohol and coumaryl alcohol (Boerjan et al. 2003, Vanholme et al. 2010). The monolignols are synthesized in the cytosol via reactions catalyzed by a number of enzymes, translocated through the plasma membrane and polymerized into lignin (Vanholme et al. 2010, Barros et al. 2015). Lignin deposition is

†These authors contributed equally to this work.

tightly orchestrated by a series of transcription factors that regulate the expression of genes involved in lignin biosynthesis during secondary wall formation (Zhong and Ye 2014). Such a transcriptional network harboring members of the NAC (NAM/ATAF/CUC) and MYB (myeloblastosis) family has been well established in Arabidopsis (Zhao and Dixon 2011, Zhong and Ye 2014). In contrast to the limited secondary growth in Arabidopsis, perennial trees exhibit predominant wood formation, and thereby conceivably possess unique regulatory mechanisms in addition to those shared by herbaceous vascular plants (Ye and Zhong 2015). Despite a few identified transcriptional regulators, the molecular network that orchestrates the dynamic regulation of xylem lignification still requires more understanding in tree species (Ye and Zhong 2015).

The MYB proteins, defined by the conserved MYB domains conferring DNA binding capability, represent a large family of transcription factors with diverse functions in eukaryotes (Dubos et al. 2010). The R2R3-type members harboring two N-terminal MYB repeats make up the largest group of the MYB family (Stracke et al. 2001). In plants, the R2R3-type MYB proteins have been identified to regulate a series of plant-specific developmental and metabolic programs (Dubos et al. 2010). Genetic and molecular evidences have revealed that a subset of MYB proteins are key regulators of secondary cell wall (SCW) formation and master components involved in SND1/NSTs/VNDs-mediated transcriptional regulation of secondary growth in plants (Zhong et al. 2008, Zhong and Ye 2014). AtMYB46 and AtMYB83 function redundantly to positively regulate SCW thickening through promoting lignin, cellulose and xylan deposition in fibers and vessels of Arabidopsis (Zhong et al. 2007, McCarthy et al. 2009). AtMYB58, AtMYB63 and AtMYB85 positively regulate lignin biosynthesis (Zhong et al. 2008, Zhou et al. 2009), while AtMYB75 represses lignin deposition (Bhargava et al. 2010). Additionally, a number of other Arabidopsis R2R3-MYB transcription factors, such as MYB52, MYB54, MYB69 and MYB103, also participate in the regulation of SCW biosynthesis (Zhong et al. 2008). Most of these SCW-associated *R2R3-MYB* genes are direct or indirect targets of some NAC transcription factors including SND1, NSTs and VNDs that act as upstream master switches of SCW thickening (Mitsuda et al. 2007, Zhong et al. 2008).

Similar R2R3-type MYB-dependent transcriptional regulation on lignin deposition and SCW formation has also been uncovered in some woody species (Zhang et al. 2014). For instance, some MYBs from *Eucalyptus* (EgMYB1 and EgMYB2) and pine (PtMYB1, PtMYB4 and PtMYB8) participate in the regulation of SCW thickening (Goicoechea et al. 2005, Bomal et al. 2008, Legay et al. 2010). The available genome sequence and the stable genetic transformation system largely facilitate the functional characterization of *R2R3-MYB* genes in *Populus* (Tuskan et al. 2006). A battery of poplar R2R3-MYB genes, including *PtrMYB3/8/20/74/75/121/128*, were identified as the downstream targets of WND (wood-associated NAC domain) transcription factors to modify wood formation (Zhong et al. 2011). PtrMYB2/3/20/21, the closest functional orthologs of Arabidopsis MYB46/83 in *Populus trichocarpa*, can bind to the SCW MYB-responsive elements (SMREs) harbored in the promoters of their targets and switch on the SCW biosynthetic program (McCarthy et al. 2010, Zhong et al. 2013). PtoMYB92 is a transcriptional activator of lignin biosynthetic pathway in *Populus tomentosa*, evidenced by the ectopic deposition of lignin during SCW development in its overexpressing poplar plants (Li et al. 2015). Heterologous expression of *PtrMYB152* and *PdMYB221* in Arabidopsis also demonstrated their roles in regulating SCW biosynthesis (Wang et al. 2014, Tang et al. 2015).

Polyploidization largely contributes to genome complexity and evolution of higher plants (del Pozo and Ramirez-Parra 2015). In monocots, due to an ancient genome-level duplication, ~50% of genes have a paralog in the modern maize genome (Schnable et al. 2011). The ancestral *Populus* genome underwent two whole-genome duplication events, one of which occurred coincidently with the split of the *Arabidopsis* and *Populus* lineages (Tuskan et al. 2006). For numerous Arabidopsis genes, a single gene usually corresponds to a pair of paralogous loci in the modern *Populus* genome (Tuskan et al. 2006). It remains elusive whether the paralogous members of these gene pairs function redundantly, cooperatively and/or specifically in poplar. To date, however, no paralogous gene pairs of poplar have been explored with respect to their common and/or divergent roles in developmental and metabolic processes.

AtMYB61, an Arabidopsis R2R3-MYB transcription factor, orchestrates multiple processes, including mucilage production, xylem lignification, root development and stomatal aperture perhaps through regulating carbon allocation (Penfield et al. 2001, Newman et al. 2004, Liang et al. 2005, Romano et al. 2012). AtMYB61 corresponds to a pair of paralogous counterparts MYB170 and MYB216 in poplar (Wilkins et al. 2009). Our previous work demonstrated that lignin was ectopically deposited in the *PtoMYB216*-overexpressing poplar plants (Tian et al. 2013). In the present study, we report molecular and functional characterization of *PtoMYB170* encoding a R2R3-MYB pleiotropic regulator in Chinese white poplar (*P. tomentosa*). Compared with its paralog PtoMYB216, PtoMYB170 exhibits conserved positive control on lignin deposition during SCW formation but unique regulation on stomata-mediated drought tolerance. These findings provide novel insights into the understanding of conserved and specific-gene function of R2R3-MYB paralogous members generated by whole-genome duplication in poplar.

## Materials and methods

### Plant materials and growth conditions

*Populus tomentosa* plants were cultivated in a greenhouse at 25 °C with 16 h 5000 lux light and 23 °C with 8 h dark.

*Arabidopsis thaliana* Col-0 seedlings were grown in a incubator at 22 °C with 16 h 10,000 lux light and 20 °C with 8 h dark. The relative humidity was kept at 60% for *P. tomentosa* and 80% for *A. thaliana*.

### Gene cloning and sequence analysis

The full-length encoding region of *PtoMYB170* (1326 bp) was amplified from *P. tomentosa* cDNA with gene-specific primers (see Table S4 available as Supplementary Data at *Tree Physiology* Online) and cloned into the pCXSN vector (Chen et al. 2009) for sequencing. Multiple sequence alignments were performed with the software DNAMAN8 (Lynnon Biosoft, San Ramon, CA, USA), and phylogenic analysis was performed with the software MEGA6.06 (Tamura et al. 2013).

### Quantitative RT-PCR

Trizol Reagent (Tiangen, Beijing, China) was used for total RNA extraction from different tissues of *P. tomentosa* plants. cDNA synthesis and quantitative RT-PCR (qRT-PCR) were performed using the PrimeScript™ RT reagent Kit (Takara, Shiga, Japan) in a TP800 Real-Time PCR machine (Takara). Expression data was normalized with reference to the transcript levels of the poplar *18S rRNA* gene. The primers for qRT-PCR analysis are listed in Table S4 available as Supplementary Data at *Tree Physiology* Online. For each gene, three biological and three technical replicates were carried out.

### Subcellular localization

The coding region (CDS) of *PtoMYB170* was inserted into the pCX-DG vector to construct a *35S-PtoMYB170:GFP* fusion via the primers Sub-*PtoMYB170*-F/R (see Table S4 available as Supplementary Data at *Tree Physiology* Online). Gene Gun GJ-1000 (SCIENTZ, Ningbo, China) was used for the bombardment of the recombinant plasmids into onion epidermal cells using. The blank vector *35S-GFP* was transformed in parallel as a control. The transiently transfected cells were stained with 4′,6-diamidino-2-phenylindole (DAPI). The GFP and DAPI fluorescent signals were detected using a confocal laser microscope (Olympus FV1200, Tokyo, Japan).

### Transactivation test in yeast

The full-length coding region of *PtoMYB170* amplified via the primers Yeast-*PtoMYB170*-F/R was inserted into the pGBKT7 vector (Clontech, Shiga, Japan) and transfected into the *Saccharomyces cerevisiae* stain Gold2. The transformed yeast cells were cultivated on Trp (tryptophan)-lacking medium for selecting positive clones and then on the TDO (triple dropout) medium without Trp, His (histidine) and Ade (adenine). X-α-gal overlay was performed to determine the transcriptional activity.

### Generation of PtoMYB170-overexpressing transgenic poplar lines

The pCXSN plasmid harboring the *PtoMYB170* coding region downstream of *CaMV 35S* promoter was transformed into *P. tomentosa* (clone 741) using the *Agrobacterium*-mediated leaf disc method as described previously (Jia et al. 2010). The positive transgenic plants were screened out via PCR with the gene-specific primers of *PtoMYB170* and hygromycin-resistant genes (see Table S4 available as Supplementary Data at *Tree Physiology* Online).

### CRISPR/Cas9-mediated mutation in poplar

The binary pYLCRIPSR/Cas9 multiplex genome targeting vector system was applied for plasmid construction of CRISPR/Cas9-mediated mutation as previously described (Fan et al. 2015, Ma et al. 2015). The coding region of *PtoMYB170* was monitored via ZiFiT Targeter (http://zifit.partners.org; Version 4.2) (Sander et al. 2010). Three putative target sites were selected for sgRNA design based on GC content (see Figure 4A). Three pairs of oligonucleotides (*PtoMYB170*-T1/2/3-F/R, see Table S4 available as Supplementary Data at *Tree Physiology* Online) were designed to specifically target *PtoMYB170* and sgRNA cassettes and constructed into the binary CRISPR/Cas9 vector via Golden Gate Cloning (Engler et al. 2009, Zhu et al. 2014). Transgenic plants harboring the *PtoMYB170*-CRISPR/Cas9 construct were produced by *Agrobacterium*-mediated transformation as described previously (Jia et al. 2010). To validate CRISPR/Cas9-mediated mutation of *PtoMYB170* in transgenic poplar plants, genomic DNA was extracted via the CTAB method, followed by PCR genotyping with the primers *PtoMYB170/216*-CAS-F and *PtoMYB170*-CAS-R (see Table S4 available as Supplementary Data at *Tree Physiology* Online). The *PtoMYB216* genomic fragment was amplified using the primers *PtoMYB170/216*-CAS-F and *PtoMYB216*-CAS-R (see Table S4 available as Supplementary Data at *Tree Physiology* Online). The amplified products were inserted into the pMD19-T Simple vector (Takara, Dalian, China) and sequenced. The leaves of *PtoMYB170*-Cas9 transgenic Line 5 were induced for calli and regenerated to produce the second generation. Similar process of PCR genotyping and DNA sequencing was performed using eight second-generation plants of Line 5. At least 20 clones were randomly selected for DNA sequencing.

### Histochemical staining and scanning electron microscope analysis

The sixth internodes of stem were cross-sectioned by hand or using an Ultra-Thin Semiautomatic Microtome (FINESSE 325, Thermo, Runcorn, UK). Histochemical staining and observation of stem cross-sections and intact leaves for lignin detection was performed as previously described (Li et al. 2015). Stem cross-sections were dissected transversely with razor blades and directly observed under scanning electron microscope (Phenomtm Pure FEI, Eindhoven, Netherland) following the manual's recommendations.

### Chemical analysis of secondary cell wall components

The total lignin content of poplar stems was quantified using Klason, acid-soluble and acetyl bromide-soluble (AcBr) lignin methods as previously described (Li et al. 2015). The absorbance was measured by a Bio UV-visible spectrophotometer (Shimadzu UV-2401 PC UV-VIS, Kyoto, Japan). An extinction coefficient of 20.0 $l\,g^{-1}\,cm^{-1}$ was applied for calculating AcBr-soluble lignin content (Wagner et al. 2007).

### Transient GUS expression measurement in tobacco leaves

Promoter sequences of four genes involved in lignin biosynthesis, including *CCR2*, *CCOAMOT1*, *COMT2* and *C4H2*, were cloned into the pCXGUS-P vector (Chen et al. 2009) to generate GUS reporter constructs. A negative reporter control harboring an 1.4 kb promoter fragment of *PtrWRKY89* was constructed (Jiang et al. 2016). The *35S-PtoMYB170* construct was used as an effector. The leaves of transgenic *Nicotiana tabacum* plants harboring *35S-PtoMYB170* were infiltrated by *Agrobacterium* harboring the reporter constructs (Sparkes et al. 2006). The GUS activity was quantitatively assayed by a spectrophotometer (F-7000, Hitachi, Tokyo, Japan) with the 365 nm excitation and the 455 nm emission filters as described previously (Jefferson 1987). Protein concentration was determined using the Bradford method (Bradford 1976).

### GUS staining driven by the PtoMYB170 promoter in Arabidopsis

A 1.8 kb fragment upstream of *PtoMYB170* start cordon was amplified from DNA with the primers Pro-*PtoMYB170*-F/R (see Table S4 available as Supplementary Data at *Tree Physiology* Online) and inserted into the pCXGUS-P vector (Chen et al. 2009). The floral dip method was used for stable transformation into Arabidopsis Col-0 plants (Clough and Bent 1998). The *PtoMYB216* promoter-GUS transgenic plants were generated as previously described (Tian et al. 2013). GUS staining was performed using the 6-week-old transgenic plants (Tian et al. 2013).

### Stomatal aperture measurements

The detached leaf abaxial epidermis was incubated in the solution containing 10 mM MES-KOH and 30 mM KCl (pH 6.5) under light for 2.5 h at 20 °C. Then 2.5-h dark or 10 μm ABA treatment was performed for assaying stomatal closing. Stomatal apertures were monitored with an Olympus BX53 microscope.

### Drought treatment

For drought treatment, the 4-week-old Arabidopsis seedlings grown in pots were desiccated without watering for 2 weeks and then rewatered. The performance of Arabidopsis seedlings was recorded by images.

### Statistical analyses

The quantitative data for expression levels, GUS activities and physiological measurements were evaluated for statistical significance using one-way ANOVA. In order to guarantee that the assumptions of ANOVA were qualified, the D'Agostino and Pearson omnibus normality test was conducted to determine if the values come from a Gaussian distribution and homogeneity of variance was assayed by Bartlett's test. If significant difference had been identified via ANOVA, a post-hoc multiple comparison was performed using Tukey or Dunnett test to distinguish the pairwise samples with significant difference ($P < 0.05$).

### Gene accessions

The GenBank accession number of PtoMYB170 is KY114929. Below are the accession numbers for the other genes in this study, including PtoMYB216: JQ801749; CCOAOMT1: EU603307; CCR2: EU603310; COMT2: EU603317; C3H3: EU603301; PAL4: EU603322; HCT1: EU603313; C4H2: EU603302; CAD1: EU603306; 4CL5: EU603299; F5H2: EU603311; PtrMYB3: EEE84749; PtrMYB20: EEE87258; AtMYB83: At3g08500; EgMYB2: CAE09057; OsMYB46: AEO53060; ZmMYB46: AEO53061; AtMYB46: At5g12870; PtrMYB2: EEE84716; PtrMYB21: EEE87289; PtMYB4: AAQ62540; AtMYB61: At1g09540; AtMYB26: At3g13890; AtMYB103: At1g63910; GhMYBL1: AHW85124; PtMYB1: AAQ62541; PtrMYB55: Potri.014G111200; PtrMYB121: Potri.002G185900; PtrMYB152: ERP50362; PtoMYB092: AKO69647; AtMYB85: At4g22680; AtMYB58: At1g16490; AtMYB63: At1g79180; SbMYB60: EES05685; AtMYB32: At4g34990; AtMYB7: At2g16720; ZmMYB42: NP_001,106,009; TaMYB4: AEG64799; EgMYB1: CAE09058; AtMYB4: At4g38620; ZmMYB31: NP_001,105,949; GhMYB9: AAK19619; AtMYB75: At1g56650; AtMYB52: At1g17950; AtMYB54: At1g73410.

## Results

### PtoMYB170 is a homolog of AtMYB61 harboring typical R2R3-MYB domains

The 1326 bp full-length ORF sequence of *PtoMYB170* encoding a 48.5 kDa protein was isolated from the cDNA of *P. tomentosa*. The PtoMYB170 protein shares an overall identity of 85% with PtoMYB216, its duplicate counterpart in the poplar genome. Multiple sequence alignment with some classical R2R3-MYB transcription factors reveals that PtoMYB170 contains typical R2- and R3-type MYB repeat domains with a Helix-Turn-Helix (HTH) motif at its N-terminus and a highly variable C-terminal region (Figure 1A). In agreement with the previous report (Wilkins et al. 2009), the phylogenetic relationship among a number of known SCW-associated R2R3-MYB transcription factors indicates that AtMYB61 is the closest homolog of the PtoMYB170/216 pair in Arabidopsis (Figure 1B). These three homologous proteins share up to more than 90% identity of their R2R3-MYB domains (Figure 1A).

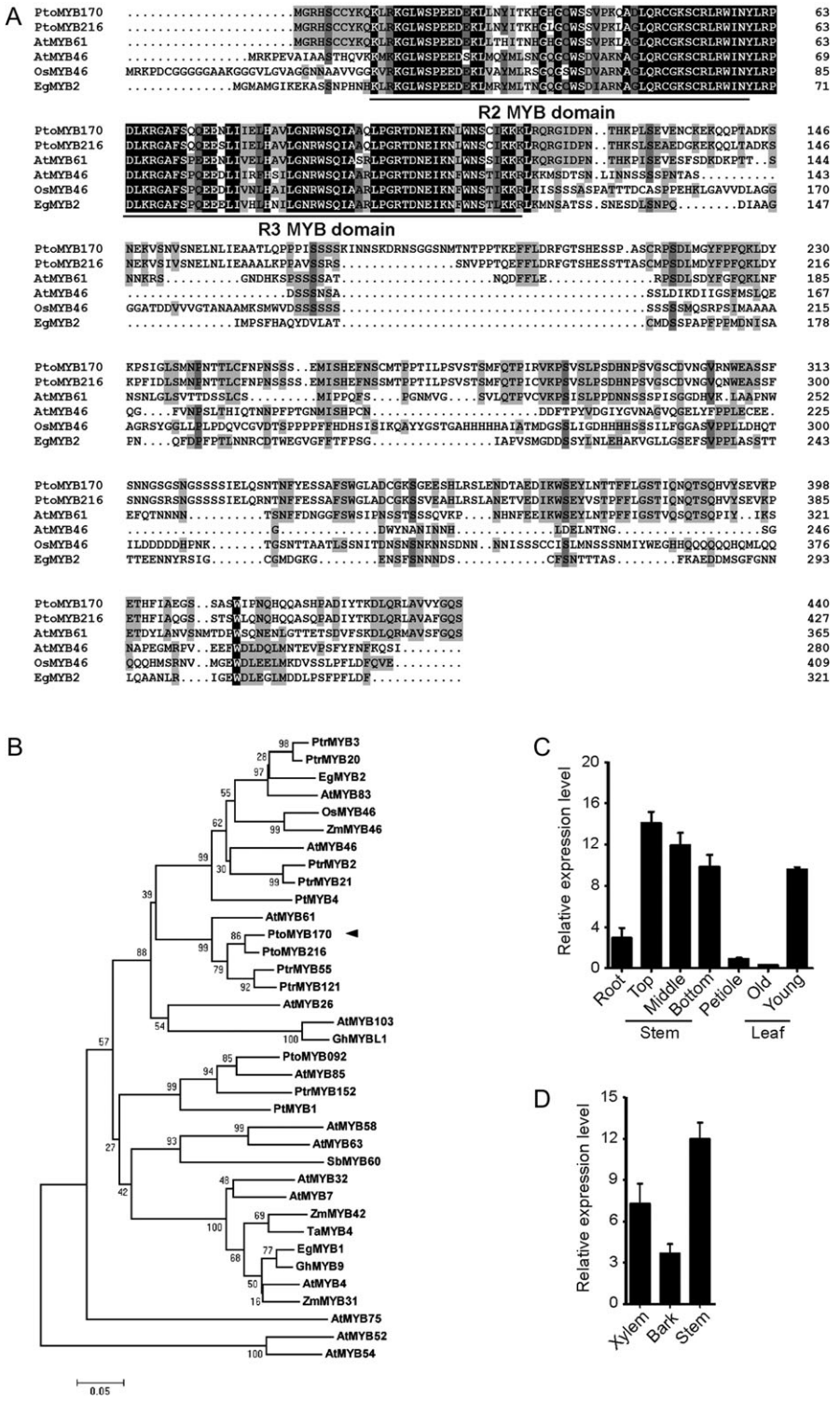


Figure 1. PtoMYB170 harbors typical R2R3-type MYB domains and displays close phylogenetic relationship with reported wood-associated MYB transcription factors. (A) Alignment of the amino acid sequences of PtoMYB170, PtoMYB216, AtMYB61 and MYB46 from rice and MYB2 from *Eucalyptus*. The PtoMYB170 protein harbors the conserved R2R3-type MYB domains that are underlined, in parallel with the other MYB transcription factors. Identical and similar amino acid residues are shaded with black and gray, respectively. (B) Phylogenetic relationship of PtoMYB170 with a number of known secondary wall-associated MYB transcription factors. The bootstrap values are indicated as percentages at the nodes. Bar = 0.05 substitutions per site. The black triangle points out the position of PtoMYB170. (C) Expression of *PtoMYB170* in seven different tissues of *P. tomentosa* plants determined by qRT-PCR. (D) Preferential expression of *PtoMYB170* in xylem of *P. tomentosa* stem assayed by qRT-PCR. Error bars: + SD. The different small letters above bars indicate significantly differential gene expression evaluated by one-way ANOVA analysis and post-hoc Tukey test for every pairwise comparison among the expression levels in tissues ($P < 0.05$).

### *Preferential expression of* PtoMYB170 *in young leaves and xylem tissues of stem*

Transcript abundance of *PtoMYB170* was determined by qRT-PCR in a series of distinct tissues of *P. tomentosa* plants (Figure 1C). *PtoMYB170* was highly expressed in stem and young leaf tissues (Figure 1C). In contrast, it exhibited relatively low expression levels in roots, petioles and mature leaves (Figure 1C). Further detection in the separated stem tissues indicated that *PtoMYB170* was preferentially expressed in xylem compared with bark (Figure 1D).

### *PtoMYB170 acts as a nucleus-localized transcriptional activator*

To examine its subcellular localization, the *PtoMYB170-GFP* fusion gene was transiently expressed in onion epidermal cells (Figure 2A). The PtoMYB170-GFP fluorescence is present exclusively in nucleus, indicated by the co-localization with nucleus-specific DAPI staining (Figure 2A). In contrast, the GFP alone displays ubiquitous localization within the cells (Figure 2A).

A transactivation experiment was performed using GAL4/Vp16-UAS system in yeast to determine the transcriptional capability of the PtoMYB170 protein (Figure 2B). The yeast cells expressing the recombinant PtoMYB170 protein fused with GAL4 DNA binding domain (GAL4BD) were grown normally on the selective medium and turned blue after overlaid with X-gal (Figure 2B). It was similar to the GAL4BD-VP16 positive control while different from the negative control transformed with GAL4BD alone. These results suggest that PtoMYB170 is a nuclear protein with the ability to activate downstream gene expression.

### *Overexpression of* PtoMYB170 *leads to morphological changes in poplar*

For functional identification, *PtoMYB170* was overexpressed in *P. tomentosa* driven by the cauliflower mosaic virus (CaMV) *35S* promoter. Three independent overexpressing lines (*PtoMYB170*-OE) with high expression levels of *PtoMYB170* quantified via qRT-PCR were selected for further analysis (Figure 3A). Compared with the wild-type, the 6-month-old transgenic plants overexpressing *PtoMYB170* displayed morphological phenotypes including retarded growth, smaller leaf size and slightly downward curled leaf blade (Figure 3B and C). Quantitative data revealed that the stem diameter of the seventh internode, plant height and leaf size were significantly attenuated in the *PtoMYB170*-OE plants (Figure 3D and E, and see Figure S2A available as Supplementary Data at *Tree Physiology* Online).

### *Pleiotropic developmental defects of CRISPR/Cas9-generated* PtoMYB170 *mutants*

The mutant lines of *PtoMYB170* were generated using the CRISPR/Cas9-based genome editing system. The sgRNA-targeted sites were assigned at three 20 bp genomic stretches followed by trinucleotide protospacer adjacent motif (PAM; 5′-NGG-3′/5′-CCN-3′) within the exons of *PtoMYB170* (Figure 4A). Genotyping analysis indicates that aberrant PCR products were amplified from 9 out of 14 transgenic lines harboring the Cas9-sgRNAs construct (Figure 4A). Compared with the single 912 bp PCR product of the wild-type, additional PCR products of smaller size were amplified from the *PtoMYB170*-Cas9 Lines 2, 5, 7–10 and 12–14 (Figure 4A), indicating the occurrence of fragment deletion. According to the size of these additional PCR products, the largest fragment deletion was present in Line 5 while the smallest in Line 2 (Figure 4A). PCR products from Lines 2, 5 and 8 were chosen for DNA sequencing. The results showed a number of mutations, including deletions, insertions and substitutions, among the three sgRNA-targeted sites of these lines (Figure 4A). Consistent with the size of their additional PCR products, a fragment deletion of 124 bp happened in Line 2, 396 bp in Line 5 and 331 bp in Line 8 (Figure 4A). A single-nucleotide

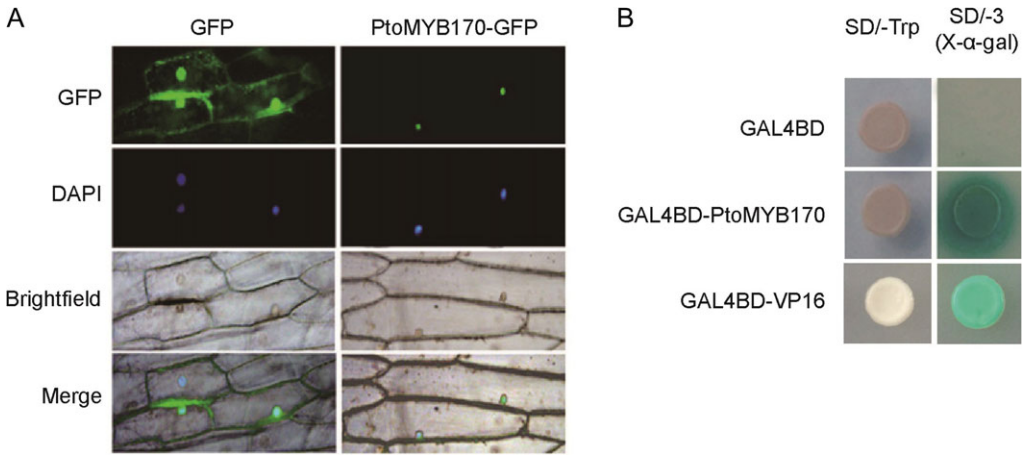


Figure 2. Subcellular localization and transactivating capability of the PtoMYB170 protein. (A) Nuclear localization of PtoMYB170 detected via transient expression in onion bulb epidermal cells. The nucleus was indicated by DAPI staining. Blank vector *35S-GFP* was used as control. (B) Transactivation capability of PtoMYB170 assayed in yeast cells. The GAL4BD-PtoMYB170 fusion enables the transformed yeast cells to grow on the selective medium lacking adenine, histidine and tryptophan (SD/-AHT) and turn blue after X-α-gal overlay.

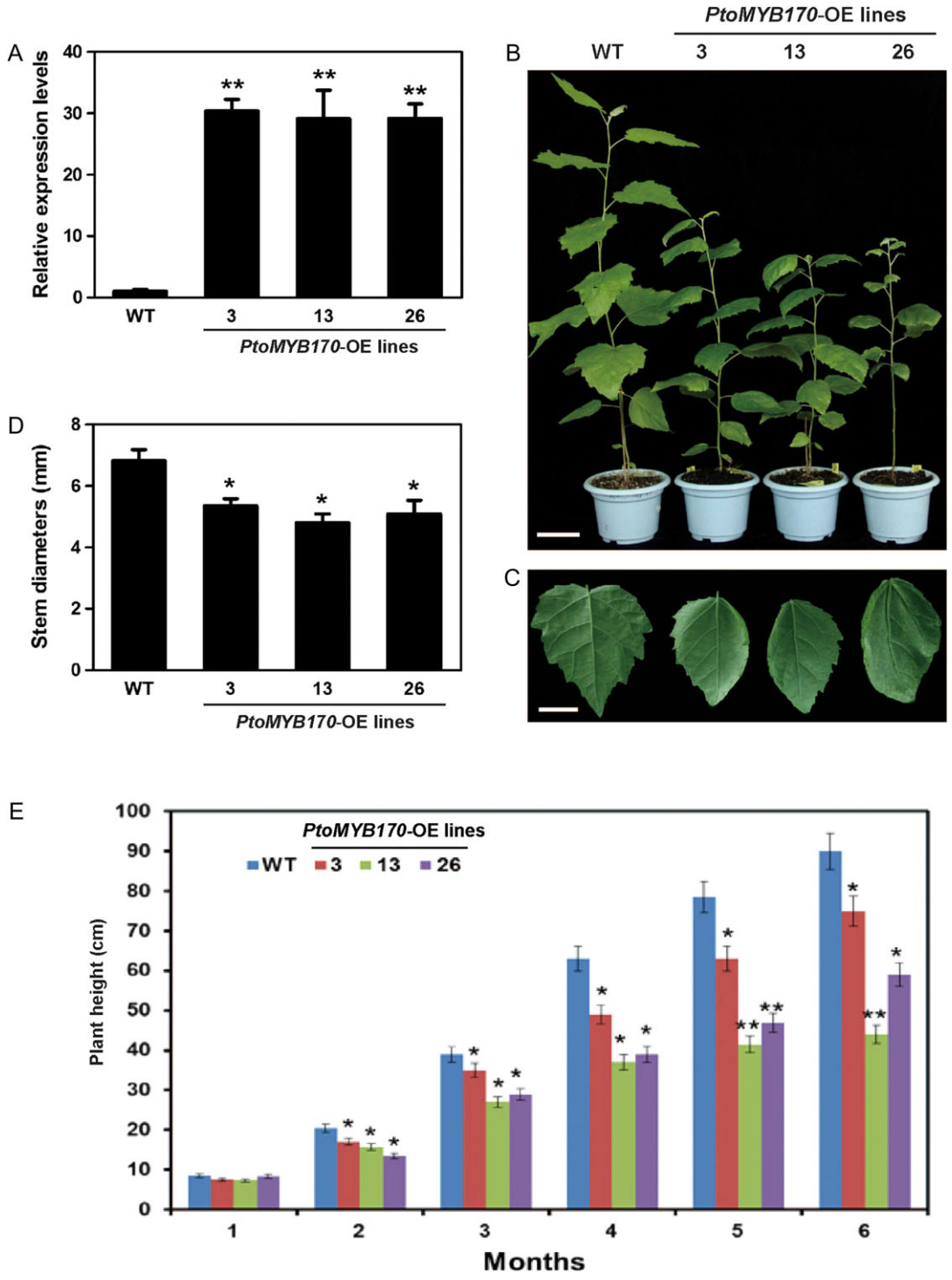


Figure 3. Morphological phenotypes of the *PtoMYB170*-overexpressing poplar lines. (A) Expression level of *PtoMYB170* in three independent transgenic lines (Line 3, 13 and 26). The poplar *18S rRNA* gene was used as an internal control. (B and C) Morphological changes of the 6-month-old *PtoMYB170*-overexpressing transgenic plants (B) and leaves (C). Scale bars = 10 cm (B) and 5 cm (C). (D and E) Measurement of stem diameter of the seventh internode (D) and plant height (E) in the wild-type and *PtoMYB170*-overexpressing lines. Error bars: ±SD. Significant differences were determined via one-way ANOVA analysis and post-hoc Dunnett test for pairwise comparison between wild-type and each *PtoMYB170*-overexpressing line (*$P < 0.05$; **$P < 0.01$).

substitution of adenine by thymine also took place in Line 2 (Figure 4A). An inversion of a 330 bp fragment occurred in Line 8 between the second and the third targeted region (Figure 4A). The insertions and deletions of one or a few nucleotides detected in all three lines led to translational frame-shift or premature termination of *PtoMYB170* (Figure 4A). To determine the stability of

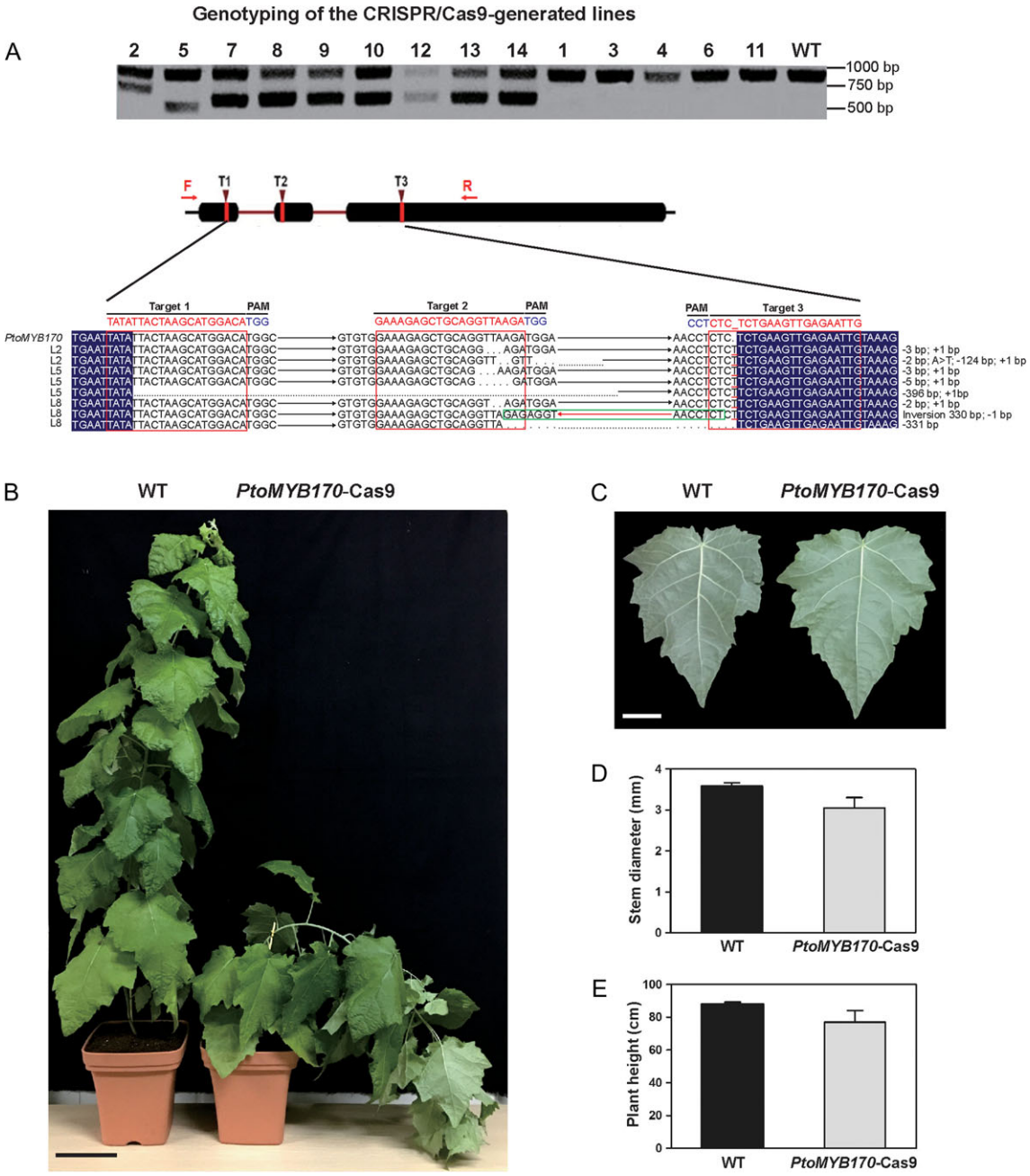


Figure 4. Creation and pleiotropic phenotypes of the CRISPR/Cas9-generated *PtoMYB170* mutant. (A) Identification of the mutations in the coding region of *PtoMYB170* generated by CRISPR/Cas9-based genome editing system. T1, T2 and T3 indicate the positions of sgRNA-targeted sites. F and R indicate the binding positions of forward and reverse primers used for PCR genotyping. The sequences of the sgRNA-targeted sites were surrounded by red boxes. The PAM sequences are in light blue. The conserved sequences are indicated in dark blue. The insertions and substitutions are underlined in red. The inversion is boxed in green. The text on the right summarizes mutation details in three independent CRISPR/Cas9-generated lines. (B and C) Morphological changes of the CRISPR/Cas9-generated *PtoMYB170* mutant plants (B) and leaves (C). Scale bars = 10 cm (B) and 5 cm (C). (D and E) Measurement of stem diameter (D) and plant height (E) in the wild-type and CRISPR/Cas9-generated *PtoMYB170* mutant. Error bars: +SD.

heritable targeted mutagenesis in transgenic poplar, the PCR products amplified from the randomly selected eight clonal progenies of Line 5 were cloned for sequencing (see Figure S1A and B available as Supplementary Data at *Tree Physiology* Online). Identical small deletions and insertions were detected in the large-size PCR fragments (the upper band) and a 396-bp fragment deletion was also found in all clonal progenies of Line 5 (see Figure S1B available as Supplementary Data at *Tree Physiology* Online). Notably, all of the 20 large-size PCR product-harbored clones randomly selected for sequencing contained mutations. Due to their close phylogenetic relationship, a 874 bp genomic fragment of *PtoMYB216* was amplified from the *PtoMYB170*-Cas9

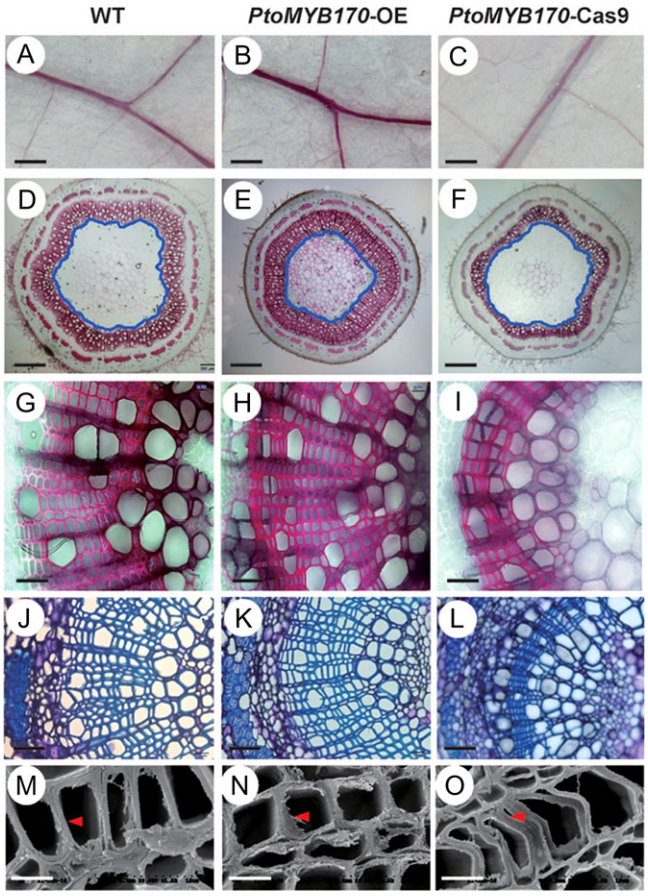


Figure 5. *PtoMYB170*-dependent regulation on lignin deposition and secondary wall development during wood formation in poplar. Leaves and cross-sections of the sixth stem internode were stained with phloroglucinol-HCl from 6-month-old wild-type (A, D and G), *PtoMYB170* overexpressing (B, E and H) and CRISPR/Cas9-generated mutant (C, F and I) plants. Cross-sections of the sixth stem internode were stained with toluidine blue from 6-month-old wild-type (J), *PtoMYB170* overexpressing (K) and CRISPR/Cas9-generated mutant (L) plants. Secondary walls of the sixth stem internode were observed with scanning electron microscopy in the wild-type (M), *PtoMYB170* overexpressing (N) and CRISPR/Cas9-generated mutant (O) plants. The red triangles point at representative thickened secondary walls of these lines (M, N and O). Scale bars = 2 mm (A, B and C), 500 μm (D, E and F), 50 μm (G, H and I), 100 μm (J, K and L) and 10 μm (M, N and O).

mutant lines for sequencing via a pair of specific primers (see Table S4 available as Supplementary Data at *Tree Physiology* Online). No mutations were detected within the coding region of *PtoMYB216* (data not shown), suggesting the specificity of CRISPR/Cas9-generated mutations for *PtoMYB170*. Taken together, these results indicate the successful generation of *PtoMYB170* loss-of-function mutant using CRISPR/Cas9-based genome editing approach despite different allelic mutations.

The *PtoMYB170*-Cas9 mutant plants, represented by Line 5, displayed a pendent stem phenotype (Figure 4B, and see Figure S1C available as Supplementary Data at *Tree Physiology* Online) and larger leaf blades (Figure 4C, and see Figure S2B available as Supplementary Data at *Tree Physiology* Online) compared with the wild-type (Figure 4C). These phenotypes were shared by all three *PtoMYB170*-Cas9 mutant lines harboring large-size fragment deletion (Lines 2, 5 and 8). Quantitative analysis revealed that the stem diameter and plant height of the mutant plants were slightly attenuated, but not significantly in statistical terms (Figure 4D and E).

### *PtoMYB170 positively regulates lignin deposition during wood formation*

The xylem-preferential expression and a pendant stem phenotype of its CRISPR/Cas9-generated mutant indicated the involvement of *PtoMYB170* in the regulation of wood formation. The lignin deposition and SCW formation were thereby determined in the vascular tissues of transgenic *PtoMYB170*-OE plants and *PtoMYB170*-Cas9 mutant (Figure 5). The lignin-specific histochemical staining showed that the strengthened lignification occurred in the leaf vasculature of the *PtoMYB170*-OE plants compared with the wild-type, whereas less lignin was deposited in that of the *PtoMYB170*-Cas9 mutant (Figure 5A). The cross-sections in stems revealed that the ectopic lignin deposition during secondary xylem growth was induced by the *PtoMYB170* overexpression, whereas it was inhibited by its CRISPR/Cas9-induced mutations (Figure 5D–I). More layers of lignified xylem fiber cells were found in the *PtoMYB170*-OE plants (16 ± 1) compared with the wild-type (10 ± 2), in contrast to less in the CRISPR/Cas9-generated mutant (6 ± 1) (Figure 5G–I). Meanwhile, lignin is ectopically deposited in the pith cells of the *PtoMYB170*-OE plants, as indicated by phloroglucinol staining (Figure 5E). In comparison with the wild-type and overexpressing plants, xylem fiber cells displayed smaller size and were more tightly arranged in the *PtoMYB170*-Cas9 mutant (Figure 5J–L). Scanning electronic microscopy revealed that the vessel cell walls of the *PtoMYB170*-OE plants were significantly thicker than those of wild-type, confirmed by the quantitative data (Figure 5M and N, and see Figure S3 available as Supplementary Data at *Tree Physiology* Online). Although the cell thickness of vessels displayed no difference, the phenotype of severely collapsed SCW was detected in the xylem tissues of the *PtoMYB170*-Cas9 mutant compared with WT (Figure 5M and O, and see Figure S3 available as Supplementary Data at *Tree Physiology* Online). These results indicated that the overexpression of *PtoMYB170* resulted in an increase of SCW thickening in xylem and ectopic deposition of lignin.

In order to quantify lignin modifications, lignin content was examined in transgenic lines via both AcBr and Klason methods. The results showed, compared with the wild type, a 7–13% increase in lignin content in the *PtoMYB170*-OE lines (see Table S1 available as Supplementary Data at *Tree Physiology* Online) and 8–12% reduction in its *PtoMYB170*-Cas9 mutant (see Table S2 available as Supplementary Data at *Tree Physiology* Online), consistent with the observation via lignin-specific histochemical staining.

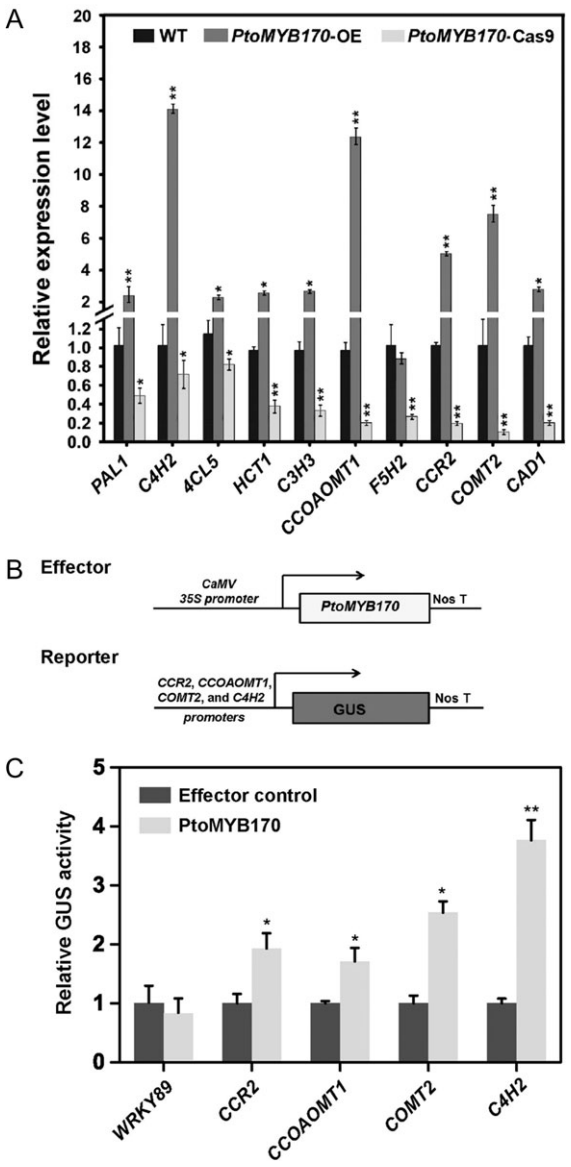


Figure 6. PtoMYB170-dependent transcriptional activation of lignin biosynthetic gene expression. (A) Expression analysis of lignin biosynthetic genes, including *PAL4*, *C4H2*, *4CL5*, *HCT*, *C3H3*, *CCOAOMT1*, *F5H2*, *CCR2*, *COMT2* and *CAD1*, in the wild-type, *PtoMYB170*-overexpressing and CRISPR/Cas9-generated mutant plants. The poplar *18S rRNA* gene was used as an internal control. One-way ANOVA analysis was performed to evaluate statistical significance of differential expression for each gene. A following Dunnett test was conducted for pairwise comparison of expression levels between wild-type and *PtoMYB170*-overexpressing lines or CRISPR/Cas9-generated mutants, respectively (*$P < 0.05$; **$P < 0.01$). (B) Schematic diagrams of the effector and reporter constructs used for transactivation analysis. The effector construct harbors the *PtoMYB170* coding region driven by the 35S promoter. The reporter construct contains the GUS reporter gene driven by the promoters of poplar CCR2, CCOAOMT1, COMT and C4H2 genes. (C) The PtoMYB170-activated expression of lignin biosynthetic genes. The effector and reporter constructs were co-transfected via *Agrobacterium*-mediated infiltration into tobacco leaf epidermal cells for GUS activity measurement. The blank effector without the *PtoMYB170* coding region was used as negative effector control. A negative reporter control harboring an 1.4 kb promoter fragment of *PtrWRKY89* was included. Error bars: ±SD from three biological repeats. For each promoter, one-way ANOVA analysis followed by Dunnett test was conducted for identifying statistical significance between the relative GUS activities driven by effector plasmids of control and *PtoMYB170* (*$P < 0.05$; **$P < 0.01$).

### *PtoMYB170 activates gene expression of lignin biosynthetic enzymes*

To further investigate the role of PtoMYB170 in the regulation of SCW biosynthesis, we determined the expression levels of the key genes encoding lignin biosynthesis-associated enzymes in transgenic plants. Among of them, most of lignin biosynthetic genes, including *PAL4*, *C4H2*, *4CL5*, *HCT*, *C3H3*, *CCOAOMT1*, *CCR2*, *COMT2* and *CAD1*, were significantly up-regulated in the *PtoMYB170*-OE plants while down-regulated in the CRISPR/Cas9-generated mutants, compared with the wild-type (Figure 6A). The expression of *F5H2* was significantly reduced in the *PtoMYB170*-Cas9 lines but not enhanced in the *PtoMYB170*-OE plants (Figure 6A).

Promoter analysis revealed that a number of SMREs, the potential DNA binding sites for MYB transcription factors, are harbored within the 1.4–2 kb region upstream of the *CCR2*, *CCOAOMT1*, *COMT* and *C4H2* genes (see Table S3 available as Supplementary Data at *Tree Physiology* Online). Therefore, the *PtoMYB170*-dependent positive regulation on lignin biosynthetic gene expression was further identified by transactivation assays in transiently expressed tobacco leaves (Figure 6B and C). The effector construct contained the *PtoMYB170* gene under the control of *CaMV 35S* promoter and the reporter constructs carried the *GUS* reporter gene driven by the promoters of lignin biosynthetic genes, including *CCR2*, *CCOAOMT1*, *COMT* and *C4H2* (Figure 6B). GUS activity measurement revealed that PtoMYB170 activated the GUS expression driven by the promoters of *CCR2*, *CCOAOMT1*, *COMT* and *C4H2* by ~1.9-, 1.7-, 2.5- and 3.8-fold, respectively (Figure 6C). These results indicated that PtoMYB170 is able to activate the expression of lignin biosynthetic genes.

### PtoMYB170 *is specifically expressed in guard cells and stimulates dark-induced stomatal closure in transgenic Arabidopsis*

As reported previously, *AtMYB61* was specifically expressed in leaf guard cells and regulated stomatal aperture in Arabidopsis (Liang et al. 2005). To investigate the expression patterns of paralogous *PtoMYB170* and *PtoMYB216*, the *GUS* reporter gene driven by their promoters were transformed into Arabidopsis, respectively. As shown in Figure 7A and Figure S3A available as Supplementary Data at *Tree Physiology* Online, GUS activity was detected in transgenic leaves carrying the promoters of these two paralogous members. The detailed observations clearly indicated that *PtoMYB170* displayed the specific expression in guard cells surrounding stomata (Figure 7B and C), whereas similar GUS staining was not detected in the leaves of transgenic

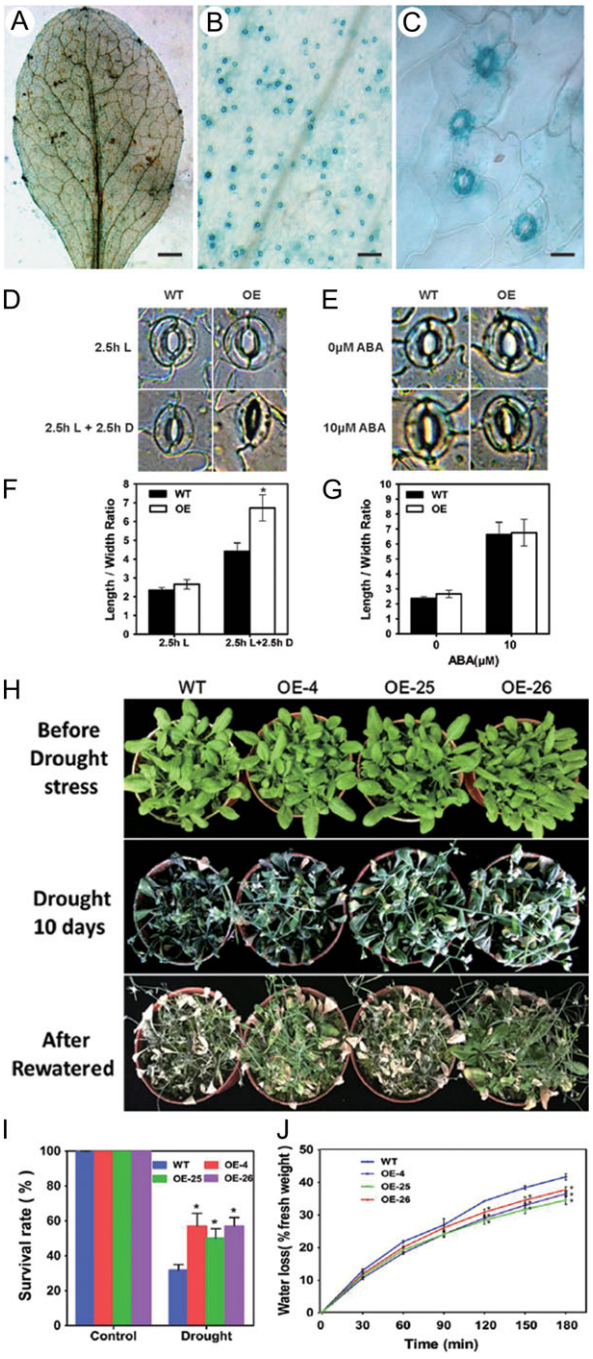


Figure 7. PtoMYB170 displays guard-cell-specific expression and confers drought tolerance in transgenic Arabidopsis. (A–C) The specific expression of *PtoMYB170* in the guard cells of Arabidopsis young leaves indicated by the GUS staining driven by its promoter. (D–G) Stomatal aperture measurements in epidermal strips with the exposure to 2.5-h dark (D and F) and 10 μm ABA (E and G) derived from wild-type and *PtoMYB170* heterologously expressed plants. (H) The representative wild-type and *PtoMYB170* heterologously expressed plants after 10-day cessation of irrigation and the following rewatering. (I) The survival rate of the wild-type and *PtoMYB170* heterologously expressed Arabidopsis plants subject to 10-day cessation of irrigation. (J) Time-course measurement of water loss in excised leaves from the wild-type and *PtoMYB170* heterologously expressed lines, indicated by percentage of the initial fresh weight at intervals. Error bars: ±SD from three biological repeats. Significant differences were calculated via one-way ANOVA analysis and post-hoc Dunnett test for pairwise comparison between wild-type and each *PtoMYB170*-overexpressing Arabidopsis line (*$P < 0.05$).

*PtoMYB216 promoter:GUS* plants (see Figure S4B and C available as Supplementary Data at *Tree Physiology* Online). The specific expression of *PtoMYB170* in guard cells implies functional diversification from its paralogous gene *PtoMYB216* in stomata-associated regulation.

Given the guard cell specific expression, the potential role of *PtoMYB170* in dark/light- and ABA-induced stomatal movement was determined in transgenic Arabidopsis overexpressing *PtoMYB170* (*PtoMYB170*-OE) (Figure 7D–G). Despite the similar stomata size to wild-type under light, the heterologous expression of *PtoMYB170* led to smaller stomatal aperture in response to dark in transgenic plants (Figure 7D and F). In contrast, no difference in stomatal aperture was observed between *PtoMYB170*-OE plants and the wild-type in response to ABA (Figure 7E and G). These results showed the specific capability of *PtoMYB170* to promote the dark-responsive stomatal closure.

### PtoMYB170 *heterologous expression enhances drought tolerance in Arabidopsis*

Because of the key roles of stomatal aperture in water loss control, drought tolerance was examined in *PtoMYB170* heterologously expressed Arabidopsis (Figure 7H–J). Transgenic lines harboring *PtoMYB170* exhibited less inhibition on growth and easier recovery than the wild-type after being subjected to drought stress for 10 days (Figure 7H). In contrast, heterologous expression of *PtoMYB216* did not confer the transgenic plants tolerance to drought stress (see Figure S4D available as Supplementary Data at *Tree Physiology* Online). Quantitative data showed the significantly higher survival rate of transgenic *PtoMYB170*-OE lines under drought treatment than the wild-type (Figure 7I). A time-course survey revealed that the *PtoMYB170*-OE lines displayed significantly decreased water loss within 3 h of desiccation compared with the wild-type (Figure 7J). Taken together, PtoMYB170 might function as a pleiotropic regulator of multiple aspects such as lignin biosynthesis and drought tolerance, but its paralog PtoMYB216 is mainly involved in the regulation of lignin biosynthetic pathway during wood formation.

## Discussion

Polyploidization is a key factor for the complexity of modern poplar genome (Tuskan et al. 2006). At least 192 genes are annotated as the members of the R2R3-MYB transcription factor family, in which a large amount of paralogous gene pairs are present due to whole-genome duplication (Wilkins et al. 2009). However, functional specificity and redundancy of paralogous MYB members have been hardly explored in poplar so far.

*PtoMYB170* and *PtoMYB216* are duplicate paralogs that correspond to a common counterpart *MYB61* in the Arabidopsis genome (Wilkins et al. 2009). Our results reveal the positive regulation of *PtoMYB170* on lignin deposition during secondary wall formation, in agreement with our previous report that *PtoMYB216* leads to ectopic lignin deposition in heterologously expressed poplar (Tian et al. 2013). These results highlight the conserved functions of *PtoMYB170/216* paralogs in regulating lignin deposition during wood formation in poplar. The functional similarity was reported among the homologous pairs of MYB transcription factors in poplar, for example, MYB2/3/20/21 (McCarthy et al. 2010, Zhong et al. 2013). However, due to the difficulty of mutant generation in poplar, functional redundancy of MYB transcription factors was rarely studied. In the present study, the CRISPR/Cas9-generated mutant of *PtoMYB170* displays pendent stem phenotype resulting from attenuated lignin deposition and more flexible SCW of xylem fibers (Figures 4 and 5). This phenomenon suggests that *PtoMYB216* is not able to replace the function of *PtoMYB170* in lignin deposition. Therefore, we speculate that weak functional redundancy during wood formation is present between the *PtoMYB170/216* paralogs in poplar.

Functional diversification between paralogous genes has been reported in plants. For instance, differential expression and imprinting of the maize paralogs *fie1* and *fie2* genes confer diversified functions in endosperm and embryo development (Danilevskaya et al. 2003). Similarly, distinct roles for the paralogous LBD transcription factors RTCS and RTCL were identified during maize shoot-borne root development (Xu et al. 2015). However, little information has been reported about functional comparison of genes in poplar. The contrasting expression in guard cells give cues to the functional divergence of *PtoMYB170/216*. *PtoMYB170* is capable of improving drought tolerance of transgenic Arabidopsis, whereas *PtoMYB216* is not. Therefore, the paralogous *PtoMYB170/216* genes function similarly in wood formation, but not redundantly, and *PtoMYB170* exhibits unique regulation on coordinating stomatal aperture with drought tolerance.

For the previously reported wood-associated *MYB* genes in poplar, the molecular evidence for their regulation on wood development were usually obtained from transgenic Arabidopsis or poplar (Tian et al. 2013, Zhong et al. 2013, Wang et al. 2014, Li et al. 2015, Tang et al. 2015). In the present study, to investigate its role in SCW biosynthesis, we generated not only the transgenic plants overexpressing *PtoMYB170* (Figure 3), but also the *PtoMYB170* mutant via CRISPR/Cas9-mediated genome editing tools to facilitate more valid evidence for its accurate gene function (Figure 4). In recent years, the CRISPR/Cas9-based genome editing system has been successfully applied for functional genomic studies in poplar (Fan et al. 2015, Zhou et al. 2015). The CRISPR/Cas9-generated mutant plants of two *4-coumarate:CoA ligase (4CL)* genes involved in lignin and flavonoid biosynthesis uniformly displayed the expected phenotypes (Zhou et al. 2015), clearly indicating the high efficiency and specificity of this editing system in poplar. In our previous study, the CRISPR/Cas9-based mutagenesis for a *phytoene desaturase (PDS)* gene was created in *P. tomentosa* with ~50% frequency of mutation rate (Fan et al. 2015). Here we successfully obtained the *PtoMYB170* mutant via the CRISPR/Cas9 system with a high efficiency (Figure 4), supporting the extensive application of the CRISPR/Cas9-based genome editing system in functional identification of transcription factors in woody plants. In contrast with small indels in *4CL* mutant plants (Zhou et al. 2015), large-size deletions up to 396 bp were detected in CRISPR/Cas9-generated *PtoMYB170* mutant lines (Figure 4). It is demonstrated that the CRISPR/Cas9-mediated mutations in transgenic poplar plants were stably inherited to clonal progenies (see Figure S1 available as Supplementary Data at *Tree Physiology* Online). Consistent with its preferential expression in secondary xylem, the *PtoMYB170* CRISPR/Cas9-generated mutation in poplar results in pleiotropic wood-associated phenotypes and remarkable changes in xylem lignification (Figure 5). These results strongly support the key role of *PtoMYB170* on lignin deposition during wood formation. Notably, the weakened lignification coincides with the more flexible secondary wall and irregular cell shape in xylem vessels and fibers of the CRISPR/Cas9-generated *PtoMYB170* mutant (Figure 5O), accounting for the pendent phenotype of its stems (Figure 4B). Similar phenotypes resulting from dominant repression of several SCW-associated MYB transcriptional activators (Zhong et al. 2007, Zhou et al. 2009) and overexpression of PdMYB221, a poplar MYB transcriptional repressor (Tang et al. 2015), have been reported. The positive regulation of PtoMYB170 on lignin deposition is explained by its transcriptional promotion of the genes encoding for lignin biosynthetic enzymes (Figure 6).

A number of MYB proteins play specific roles in drought tolerance via regulating various processes, for example, stomatal movement, suberin and wax synthesis, and lateral root growth (Baldoni et al. 2015). Some MYB transcription factors represented by MYB60 and MYB96 in Arabidopsis regulate stomatal opening (Cominelli et al. 2005, Seo et al. 2009), while some others including AtMYB61 and AtMYB44 are involved in stomatal pore closure (Liang et al. 2005, Jung et al. 2008). Loss-of-function and gain-of-function analysis of *AtMYB61* clearly indicates its role in promoting reductions in stomatal aperture and thereby influencing gas exchange in leaves (Liang et al. 2005). In agreement with its homolog counterpart *MYB61* in Arabidopsis, *PtoMYB170* displays the guard-cell-specific expression and increases dark-induced stomatal closure specifically. However, it is not yet reported whether *AtMYB61*-regulated stomatal aperture contributes to drought tolerance (Baldoni et al. 2015). AtMYB60, another guard-cell-specific MYB transcription factor, is able to regulate stomatal opening and drought tolerance in Arabidopsis (Cominelli et al. 2005). The heterologous expression of *PtoMYB170* confers the enhanced

tolerance to drought stress, suggesting its dual role in the regulation of stomatal aperture and drought tolerance. The reduced water loss in the *PtoMYB170* transgenic plants indicates that the increased drought tolerance may be associated with *PtoMYB170*-promoted stomatal closure. Therefore, PtoMYB170 may act as a regulator of coordinating stomatal movement and drought tolerance.

In summary, PtoMYB170 is a typical R2R3 MYB transcription factor that displays nuclear localization and transcriptional activating capability. It exhibits a close phylogenetic relationship with wood-associated MYB transcription factors and preferential expression in xylem tissues. Functional identification by both overexpression and CRISPR/Cas9-generated mutation revealed that PtoMYB170 positively regulates lignin deposition during wood formation in poplar through activating lignin biosynthetic gene expression, and uniquely acts on promoting dark-induced stomatal closure and drought tolerance in comparison with its paralog *PtoMYB216*.

## Supplementary Data

Supplementary Data for this article are available at *Tree Physiology* Online.

## Funding

This work was supported by the National Key Research and Development Program (2016YFD0600105), the National Natural Science Foundation of China (31370672, 31500216, 31500544 and 31370317), Chongqing Research Program of Basic Research and Frontier Technology (cstc2015jcyjA80036 and cstc2013jcyjA80016) and Fundamental Research Funds for the Central Universities (XDJK2016B032).

## Conflict of interest

We declare that we have no conflict of interest.

## References

Baldoni E, Genga A, Cominelli E (2015) Plant MYB transcription factors: their role in drought response mechanisms. Int J Mol Sci 16: 15811–15851.

Barros J, Serk H, Granlund I, Pesquet E (2015) The cell biology of lignification in higher plants. Ann Bot 115:1053–1074.

Bhargava A, Mansfield SD, Hall HC, Douglas CJ, Ellis BE (2010) MYB75 functions in regulation of secondary cell wall formation in the Arabidopsis inflorescence stem. Plant Physiol 154:1428–1438.

Boerjan W, Ralph J, Baucher M (2003) Lignin biosynthesis. Annu Rev Plant Biol 54:519–546.

Bomal C, Bedon F, Caron S et al. (2008) Involvement of *Pinus taeda* MYB1 and MYB8 in phenylpropanoid metabolism and secondary cell wall biogenesis: a comparative in planta analysis. J Exp Bot 59: 3925–3939.

Bonan GB (2008) Forests and climate change: forcings, feedbacks, and the climate benefits of forests. Science 320:1444–1449.

Bradford MM (1976) A rapid and sensitive method for the quantitation of microgram quantities of protein utilizing the principle of protein-dye binding. Anal Biochem 72:248–254.

Chen S, Songkumarn P, Liu J, Wang GL (2009) A versatile zero background T-vector system for gene cloning and functional genomics. Plant Physiol 150:1111–1121.

Clough SJ, Bent AF (1998) Floral dip: a simplified method for Agrobacterium-mediated transformation of *Arabidopsis thaliana*. Plant J 16:735–743.

Cominelli E, Galbiati M, Vavasseur A, Conti L, Sala T, Vuylsteke M, Leonhardt N, Dellaporta SL, Tonelli C (2005) A guard-cell-specific MYB transcription factor regulates stomatal movements and plant drought tolerance. Curr Biol 15:1196–1200.

Danilevskaya ON, Hermon P, Hantke S, Muszynski MG, Kollipara K, Ananiev EV (2003) Duplicated *fie* genes in maize: expression pattern and imprinting suggest distinct functions. Plant Cell 15:425–438.

del Pozo JC, Ramirez-Parra E (2015) Whole genome duplications in plants: an overview from Arabidopsis. J Exp Bot 66:6991–7003.

Dubos C, Stracke R, Grotewold E, Weisshaar B, Martin C, Lepiniec L (2010) MYB transcription factors in Arabidopsis. Trends Plant Sci 15: 573–581.

Engler C, Gruetzner R, Kandzia R, Marillonnet S (2009) Golden gate shuffling: a one-pot DNA shuffling method based on type IIs restriction enzymes. PLoS One 4:e5553.

Fan D, Liu T, Li C, Jiao B, Li S, Hou Y, Luo K (2015) Efficient CRISPR/Cas9-mediated targeted mutagenesis in *Populus* in the first generation. Sci Rep 5:12217.

Goicoechea M, Lacombe E, Legay S et al. (2005) EgMYB2, a new transcriptional activator from *Eucalyptus* xylem, regulates secondary cell wall formation and lignin biosynthesis. Plant J 43:553–567.

Jefferson RA (1987) Assaying chimeric genes in plants: the GUS gene fusion system. Plant Mol Biol Report 5:387–405.

Jia Z, Sun Y, Yuan L, Tian Q, Luo K (2010) The chitinase gene (Bbchit1) from *Beauveria bassiana* enhances resistance to *Cytospora chrysosperma* in *Populus tomentosa* Carr. Biotechnol Lett 32:1325–1332.

Jiang Y, Guo L, Liu R, Jiao B, Zhao X, Ling Z, Luo K (2016) Overexpression of poplar *PtrWRKY89* in transgenic Arabidopsis leads to a reduction of disease resistance by regulating defense-related genes in salicylate- and jasmonate-dependent signaling. PLoS One 11: e0149137.

Jung C, Seo JS, Han SW, Koo YJ, Kim CH, Song SI, Nahm BH, Choi YD, Cheong JJ (2008) Overexpression of AtMYB44 enhances stomatal closure to confer abiotic stress tolerance in transgenic Arabidopsis. Plant Physiol 146:623–635.

Legay S, Sivadon P, Blervacq AS et al. (2010) EgMYB1, an R2R3 MYB transcription factor from eucalyptus negatively regulates secondary cell wall formation in Arabidopsis and poplar. New Phytol 188:774–786.

Li C, Wang X, Ran L, Tian Q, Fan D, Luo K (2015) PtoMYB92 is a transcriptional activator of the lignin biosynthetic pathway during secondary cell wall formation in *Populus tomentosa*. Plant Cell Physiol 56: 2436–2446.

Liang YK, Dubos C, Dodd IC, Holroyd GH, Hetherington AM, Campbell MM (2005) AtMYB61, an R2R3-MYB transcription factor controlling stomatal aperture in *Arabidopsis thaliana*. Curr Biol 15:1201–1206.

Ma X, Zhang Q, Zhu Q et al. (2015) A robust CRISPR/Cas9 system for convenient, high-efficiency multiplex genome editing in monocot and dicot plants. Mol Plant 8:1274–1284.

McCarthy RL, Zhong R, Ye ZH (2009) MYB83 is a direct target of SND1 and acts redundantly with MYB46 in the regulation of secondary cell wall biosynthesis in Arabidopsis. Plant Cell Physiol 50:1950–1964.

McCarthy RL, Zhong R, Fowler S, Lyskowski D, Piyasena H, Carleton K, Spicer C, Ye ZH (2010) The poplar MYB transcription factors, PtrMYB3 and PtrMYB20, are involved in the regulation of secondary wall biosynthesis. Plant Cell Physiol 51:1084–1090.

Mitsuda N, Iwase A, Yamamoto H, Yoshida M, Seki M, Shinozaki K, Ohme-Takagi M (2007) NAC transcription factors, NST1 and NST3, are key regulators of the formation of secondary walls in woody tissues of Arabidopsis. Plant Cell 19:270–280.

Newman LJ, Perazza DE, Juda L, Campbell MM (2004) Involvement of the R2R3-MYB, AtMYB61, in the ectopic lignification and dark-photomorphogenic components of the *det3* mutant phenotype. Plant J 37:239–250.

Penfield S, Meissner RC, Shoue DA, Carpita NC, Bevan MW (2001) MYB61 is required for mucilage deposition and extrusion in the Arabidopsis seed coat. Plant Cell 13:2777–2791.

Ragauskas AJ, Williams CK, Davison BH et al. (2006) The path forward for biofuels and biomaterials. Science 311:484–489.

Romano JM, Dubos C, Prouse MB et al. (2012) AtMYB61, an R2R3-MYB transcription factor, functions as a pleiotropic regulator *via* a small gene network. New Phytol 195:774–786.

Sander JD, Maeder ML, Reyon D, Voytas DF, Joung JK, Dobbs D (2010) ZiFiT (Zinc Finger Targeter): an updated zinc finger engineering tool. Nucleic Acids Res 38:W462–W468.

Schnable JC, Springer NM, Freeling M (2011) Differentiation of the maize subgenomes by genome dominance and both ancient and ongoing gene loss. Proc Natl Acad Sci USA 108:4069–4074.

Seo PJ, Xiang F, Qiao M, Park JY, Lee YN, Kim SG, Lee YH, Park WJ, Park CM (2009) The MYB96 transcription factor mediates abscisic acid signaling during drought stress response in Arabidopsis. Plant Physiol 151:275–289.

Sparkes IA, Runions J, Kearns A, Hawes C (2006) Rapid, transient expression of fluorescent fusion proteins in tobacco plants and generation of stably transformed plants. Nat Protoc 1:2019–2025.

Stracke R, Werber M, Weisshaar B (2001) The R2R3-MYB gene family in *Arabidopsis thaliana*. Curr Opin Plant Biol 4:447–456.

Tamura K, Stecher G, Peterson D, Filipski A, Kumar S (2013) MEGA6: Molecular Evolutionary Genetics Analysis version 6.0. Mol Biol Evol 30:2725–2729.

Tang X, Zhuang Y, Qi G, Wang D, Liu H, Wang K, Chai G, Zhou G (2015) Poplar PdMYB221 is involved in the direct and indirect regulation of secondary wall biosynthesis during wood formation. Sci Rep 5: 12240.

Tian Q, Wang X, Li C, Lu W, Yang L, Jiang Y, Luo K (2013) Functional characterization of the poplar R2R3-MYB transcription factor PtoMYB216 involved in the regulation of lignin biosynthesis during wood formation. PLoS One 8:e76369.

Tuskan GA, Difazio S, Jansson S et al. (2006) The genome of black cottonwood, *Populus trichocarpa* (Torr. & Gray). Science 313: 1596–1604.

Vanholme R, Demedts B, Morreel K, Ralph J, Boerjan W (2010) Lignin biosynthesis and structure. Plant Physiol 153:895–905.

Wagner A, Ralph J, Akiyama T, Flint H, Phillips L, Torr K, Nanayakkara B, Te Kiri L (2007) Exploring lignification in conifers by silencing hydroxycinnamoyl-CoA:shikimate hydroxycinnamoyltransferase in *Pinus radiata*. Proc Natl Acad Sci USA 104:11856–11861.

Wang S, Li E, Porth I, Chen JG, Mansfield SD, Douglas CJ (2014) Regulation of secondary cell wall biosynthesis by poplar R2R3 MYB transcription factor PtrMYB152 in Arabidopsis. Sci Rep 4:5054.

Wilkins O, Nahal H, Foong J, Provart NJ, Campbell MM (2009) Expansion and diversification of the *Populus* R2R3-MYB family of transcription factors. Plant Physiol 149:981–993.

Xu C, Tai H, Saleem M et al. (2015) Cooperative action of the paralogous maize lateral organ boundaries (LOB) domain proteins RTCS and RTCL in shoot-borne root formation. New Phytol 207:1123–1133.

Ye ZH, Zhong R (2015) Molecular control of wood formation in trees. J Exp Bot 66:4119–4131.

Zhang J, Nieminen K, Serra JA, Helariutta Y (2014) The formation of wood and its control. Curr Opin Plant Biol 17:56–63.

Zhao Q, Dixon RA (2011) Transcriptional networks for lignin biosynthesis: more complex than we thought? Trends Plant Sci 16:227–233.

Zhong R, Ye ZH (2014) Complexity of the transcriptional network controlling secondary wall biosynthesis. Plant Sci 229:193–207.

Zhong R, Richardson EA, Ye ZH (2007) The MYB46 transcription factor is a direct target of SND1 and regulates secondary wall biosynthesis in Arabidopsis. Plant Cell 19:2776–2792.

Zhong R, McCarthy RL, Lee C, Ye ZH (2011) Dissection of the transcriptional program regulating secondary wall biosynthesis during wood formation in poplar. Plant Physiol 157:1452–1468.

Zhong R, McCarthy RL, Haghighat M, Ye ZH (2013) The poplar MYB master switches bind to the SMRE site and activate the secondary wall biosynthetic program during wood formation. PLoS One 8:e69219.

Zhong R, Lee C, Zhou J, McCarthy RL, Ye ZH (2008) A battery of transcription factors involved in the regulation of secondary cell wall biosynthesis in Arabidopsis. Plant Cell 20:2763–2782.

Zhou J, Lee C, Zhong R, Ye ZH (2009) MYB58 and MYB63 are transcriptional activators of the lignin biosynthetic pathway during secondary cell wall formation in Arabidopsis. Plant Cell 21:248–266.

Zhou X, Jacobs TB, Xue LJ, Harding SA, Tsai CJ (2015) Exploiting SNPs for biallelic CRISPR mutations in the outcrossing woody perennial *Populus* reveals 4-coumarate:CoA ligase specificity and redundancy. New Phytol 208:298–301.

Zhu QL, Yang ZF, Zhang QY, Chen LT, Liu YG (2014) Robust multi-type plasmid modifications based on isothermal in vitro recombination. Gene 548:39–42.